INL/RPT-23-74341

Multiphysics Pebble-Bed Reactor Control Rod Withdrawal Study

September 2023

M3AT-22IN0603011

Vincent Labouré[1], Paolo Balestra[1], Javier Ortensi[1], Joshua Hanophy[1], Zachary Prince[1], Ryan Stewart[1], and Gerhard Strydom[1]

[1]*Idaho National Laboratory*

INL is a U.S. Department of Energy National Laboratory operated by Battelle Energy Alliance, LLC

INL/RPT-23-74341

Multiphysics Pebble-Bed Reactor Control Rod Withdrawal Study

M3AT-22IN0603011

Vincent Labouré[1], Paolo Balestra[1], Javier Ortensi[1], Joshua Hanophy[1], Zachary Prince[1], Ryan Stewart[1], and Gerhard Strydom[1]

[1]Idaho National Laboratory

September 2023

Idaho National Laboratory
Advanced Reactor Technologies
Idaho Falls, Idaho 83415

http://www.art.inl.gov

Prepared for the
U.S. Department of Energy
Office of Nuclear Energy
Under DOE Idaho Operations Office
Contract DE-AC07-05ID14517

Page intentionally left blank

SUMMARY

This work studied the responses of both a generic gas- and a fluoride-cooled pebble-bed reactor (PBR) concept—the gPBR-200 and gFHR, respectively—during reactivity insertion accidents. Both models rely on 2-D axisymmetric simulations to solve the neutron flux distribution, nuclide concentrations, and temperature across the core—in addition to numerous representative pebble and tristructural isotropic (TRISO) particle simulations for determining fuel and moderator temperatures. This not only allows for computing maximum temperatures in the core—thus enabling estimation of how near the fuel is to peak operational and safety limits—as prescribed by specified acceptable fuel design limits, which are determined in such a way that fuel is not damaged during operational or anticipated abnormal occurrences—but also predicting how much of the core exceeds a given temperature limit, as well as determining the local energy deposition rate.

These models consider both control rod withdrawal (CRW) and control rod ejection (CRE) events. The former introduces a great deal more reactivity, as all the control rods are withdrawn (as opposed to a single one in the latter case), though at a much slower pace. In addition, for the gPBR-200, two limiting cases were considered: one with the core starting under hot full-power conditions and one with it starting under cold zero-power conditions. While the amount of reactivity added in the latter case is much higher (due to the far lower temperatures and the lack of neutron poisons such as Xe-135), the margin to temperature limits is also much more significant.

Overall, for the design considered, none of the accidents resulted in the maximum fuel temperature reaching values close to the TRISO limit. However, the methodology presented herein could be very relevant if some designs consider reduced margins (e.g., higher temperatures) to achieve enhanced economics.

Further model improvement is needed to better capture control rod worth, both in

terms of cusping effects (as the rods are slowly withdrawn) and differential worth, especially as the tips of the rods near the upper cavity.

Page intentionally left blank

CONTENTS

FIGURES

TABLES

ACRONYMS

B_4C	boron carbide
CR	control rod
CRE	control rod ejection
CRW	control rod withdrawal
PB-FHR	pebble-bed fluoride-cooled high-temperature reactor
PBR	pebble-bed reactor
TRISO	tristructural isotropic

Page intentionally left blank

1. INTRODUCTION

Advanced nuclear reactors have been the subject of renewed attention in terms of better competing with carbon-emitting energy resources. A number of these concepts, including the high-temperature reactor, utilize tristructural isotropic (TRISO) fuel particles, which can withstand extreme temperatures (on the order of 2100 K) without releasing significant quantities of fission products. However, questions have arisen as to whether certain conditions that might challenge the integrity of the TRISO particles could be encountered during reactivity insertion events in which the power density and fuel temperature rapidly increase [4, 7].

More specifically, the goal is to develop numerical models that can eventually predict how much of the core exceeds a given temperature limit and for how long, and that can calculate the local energy deposition rate—as opposed to models that rely on point kinetics with simplified thermal-hydraulics. Although best-estimate models are generally much more expensive to build and run, they can better estimate how close the reactor is to exceeding the set limits, thereby potentially enabling designs with reduced safety margins.

This work focuses on the response of a pebble-bed reactor (PBR)—a particular type of high-temperature reactor that relies on TRISO-fueled graphite pebbles that slowly circulate through the core—to such events. Two types of reactors are considered: the gPBR-200, a generic 200 MW gas-cooled PBR introduced in [18, 19], and the gFHR, a generic 280 MW pebble-bed fluoride-cooled high-temperature reactor (PB-FHR) taken from [14]. Furthermore, two types of unprotected reactivity insertion accidents (classified as "anticipated transient without scram") are considered: (1) control rod withdrawal (CRW) events (design basis accident) in which every control rod (CR) is assumed to be unintentionally removed—slowly, but entirely—and (2) control rod ejection (CRE) events (beyond design basis accident), defined as the quasi-instantaneous removal of a single CR—even though such an event may not be possible, depending on the design. These events are analyzed to demonstrate code capabilities, but, in practice, each scenarios would need to be informed by probability risk assessment to establish its likelihood of occurrence.

The remainder of this report is organized as follows. The numerical models and workflow are presented in Section 2, and the corresponding results are the subject of Section 3. Conclusions and recommendations for future work are discussed in Section 4.

2. MODEL DESCRIPTION

Within this section, the gPBR-200 and gFHR models are described in Section 2.1 and Section 2.2, respectively, and the workflows for hot full-power and cold zero-power conditions are presented in Section 2.3. Both models are very similar in that they use a 2-D axisymmetric Griffin [8, 20] model for both the neutronics and microscopic depletion to perform an equilibrium core calculation, a 2-D axisymmetric Pronghorn model that utilizes the Navier-Stokes porous media formulation [5, 6] for the full-core thermal model, and representative pebble and TRISO models (for each core zone and burnup group) to compute fuel and moderator temperature.

2.1 Gas-cooled Pebble-Bed Reactor

2.1.1 Model Overview

The generic gas-cooled PBR model (coined the "gPBR-200" for its 200 MW thermal power capability) studied in this work was first introduced in [18, 19], and its specifications were derived from various sources [1, 12, 15]. Figure 1 gives an overview of the geometry: Figure 1b shows the detailed, heterogeneous Serpent model [9] used as a reference solution (e.g., to compute CR worth), whereas Figure 1c describes the 2-D RZ simplified geometry for both Griffin and Pronghorn. One of the major approximations is that the CR channel in Figure 1c—which effectively models a "gray" curtain of absorbing material—can adequately represent the nine CRs and nine shutdown rods (in dark and light purple, respectively, in Figure 1a) drilled inside the graphite radial reflector. The azimuthal material dependence inside that curtain is, in practice, very challenging to fully capture with an axisymmetric representation.

Another challenge lies in the upper cavity's very low cross sections, as it is only filled with helium. At the time this study began, the main option in Griffin for solving a full-core RZ problem was a diffusion solver, which, in near-void regions, typically struggles to properly capture neutron streaming. The cumulative migration method [10] was thus used with Serpent in order to compute reasonable directional diffusion coefficients in the cavity.

A summary of the Griffin-Pronghorn equilibrium core model and its multiphysics coupling is

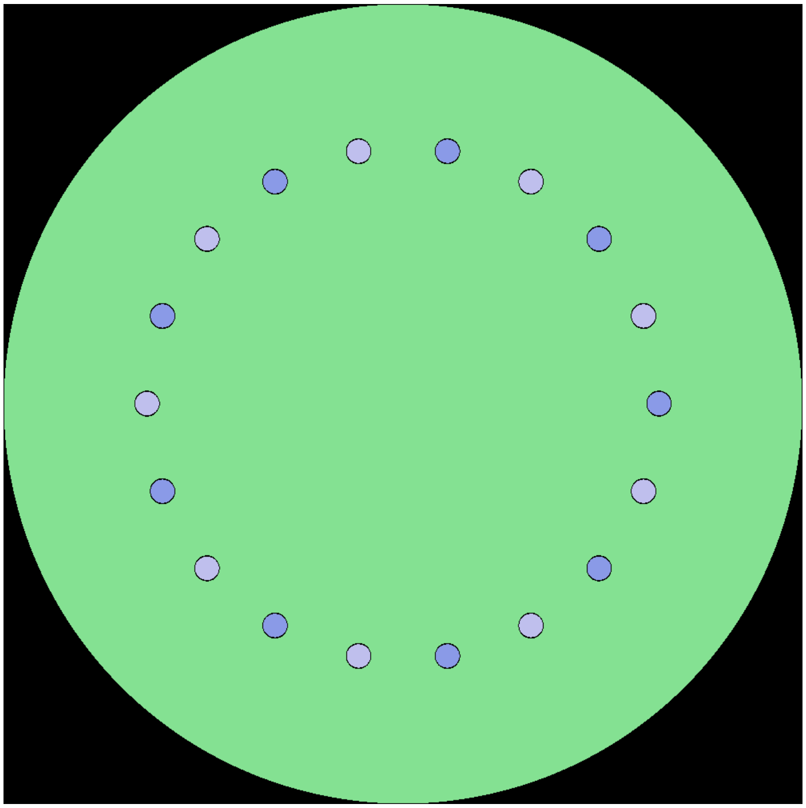

(a) 3-D Serpent geometry (top view)

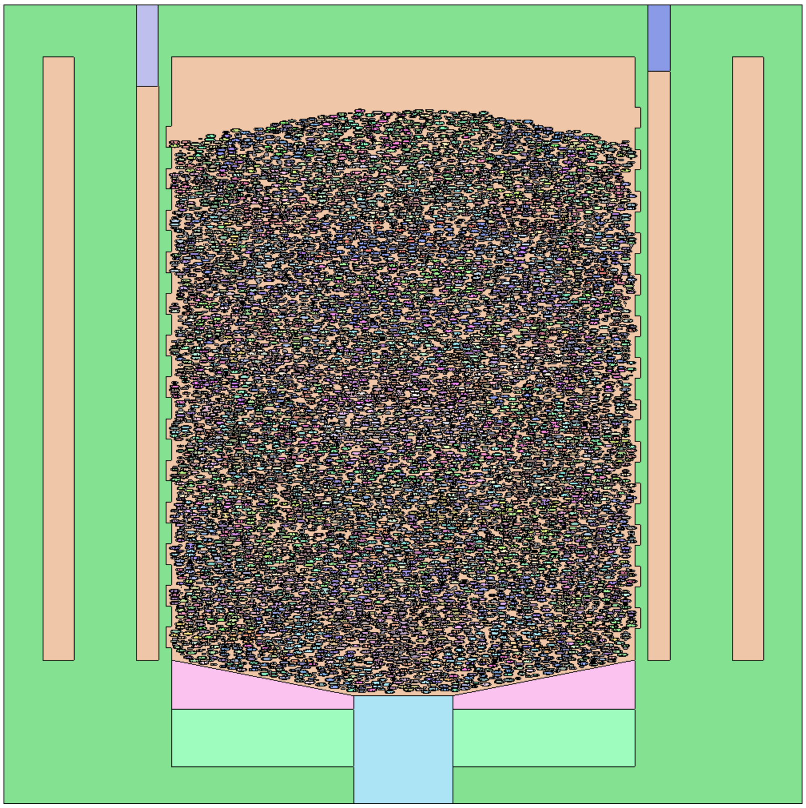

(b) 3-D Serpent geometry (axial view)

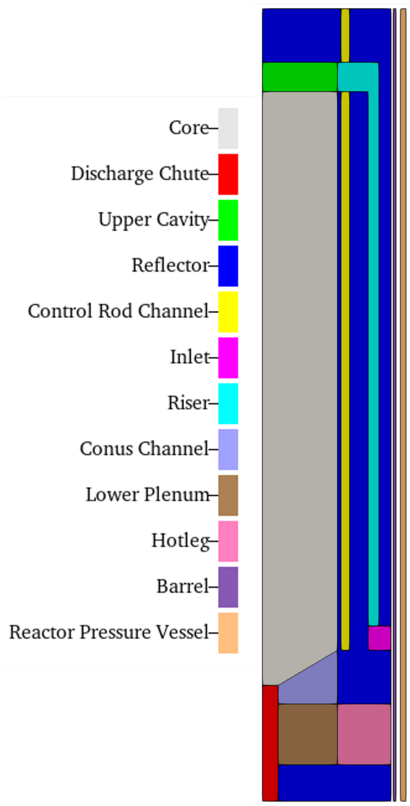

(c) 2-D RZ simplified geometry

Figure 1: Overview of the gPBR-200 geometry.

given in Figure 2. The workflow for generating the cross sections for that model and performing the transient calculations based on that equilibrium core solution are discussed in Section 2.3.

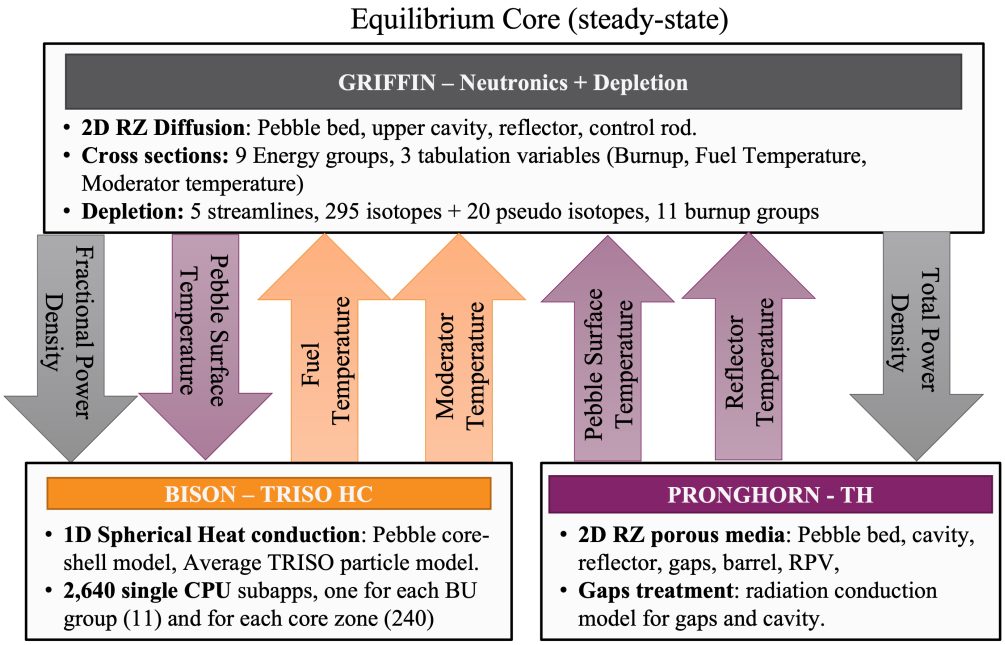

Figure 2: Multiphysics coupling for the gPBR-200 equilibrium core calculation.

2.1.2 Control Rod Worth

The CR worth of the Griffin model is given in Figure 3. Although the eigenvalue as a function of CR position looks fairly smooth, the differential worth displays some oscillations. This lack of smoothness in the reactivity curve—commonly referred to as *cusping*—persists despite the decusping treatment applied in Griffin [16]. This numerical artifact will be visible for slow CR motion over a long period of time, such as in the scenario considered in Section 3.1.3.

Another deficiency in the model is that, based on the Serpent reference reactivity curve (and unlike what is seen in Figure 3), the differential worth should not increase when the tip of the CR approaches the upper cavity. This indicates that the treatment of the upper cavity in the Griffin model should be improved in the future.

2.2 Fluoride-cooled Pebble-Bed Reactor

The generic PB-FHR model (i.e., the gFHR) used in this work comes from—and is described in great detail in—[14]. The main differences (relevant for this study) between it and the gPBR-200

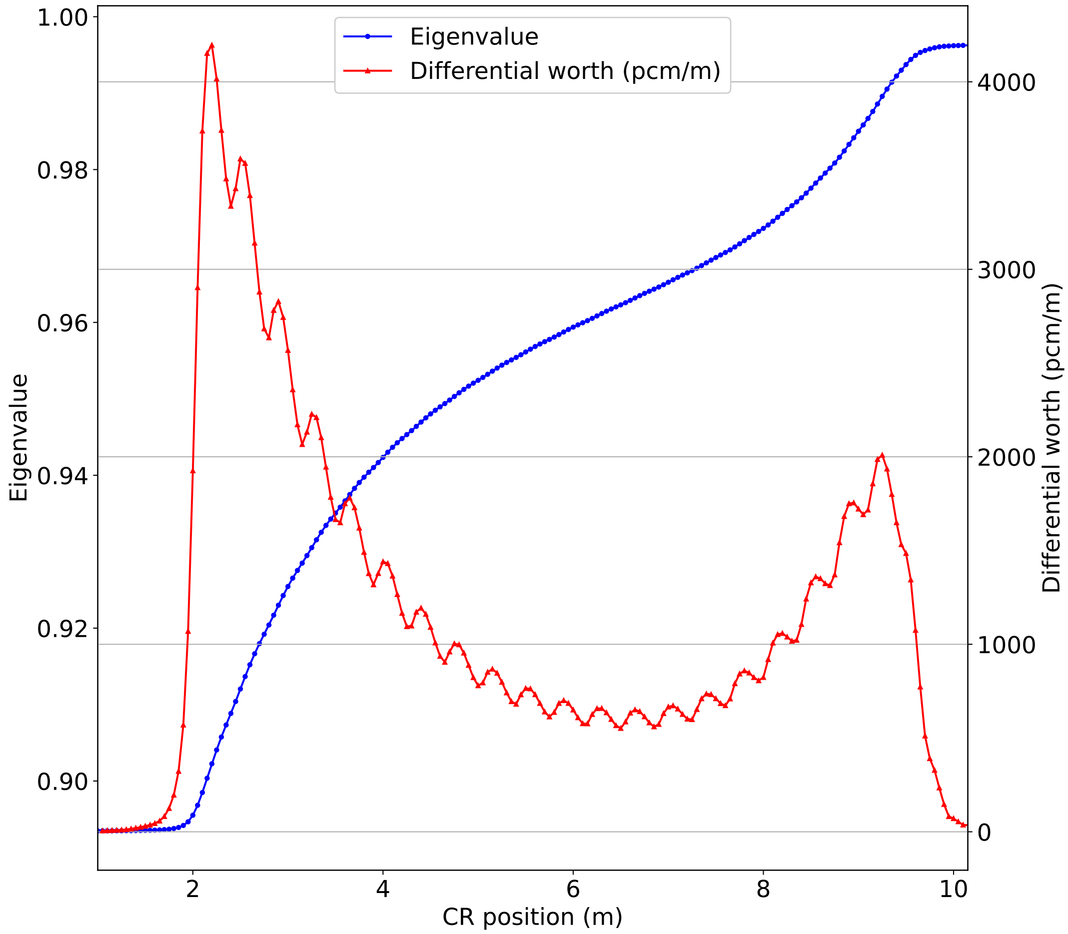

Figure 3: Reactivity curve of the gPBR-200 model under hot full-power conditions.

model are:

- The total nominal power is 280 MW instead of 200 MW.
- The coolant is FLiBe, a molten salt that contains fluoride, lithium (mostly Li-7, since Li-6 degrades neutron economy), and beryllium. Unlike helium, it is not transparent to neutrons—leading to an additional reactivity feedback mechanism due the density of FLiBe decreasing with temperature—and is solid at room temperature, meaning that the core cannot be kept in cold conditions.
- The power density is generally higher for fluoride-cooled than for gas-cooled PBRs, due to

the former's superior heat transfer coefficients.

2.2.1 Model Overview

The Griffin neutronics and streamline depletion meshes are summarized in Figure 4, whereas the Pronghorn models are shown in Figure 5. The multiphysics coupling, which is very similar to that of the gPBR-200 model, is given in Figure 6.

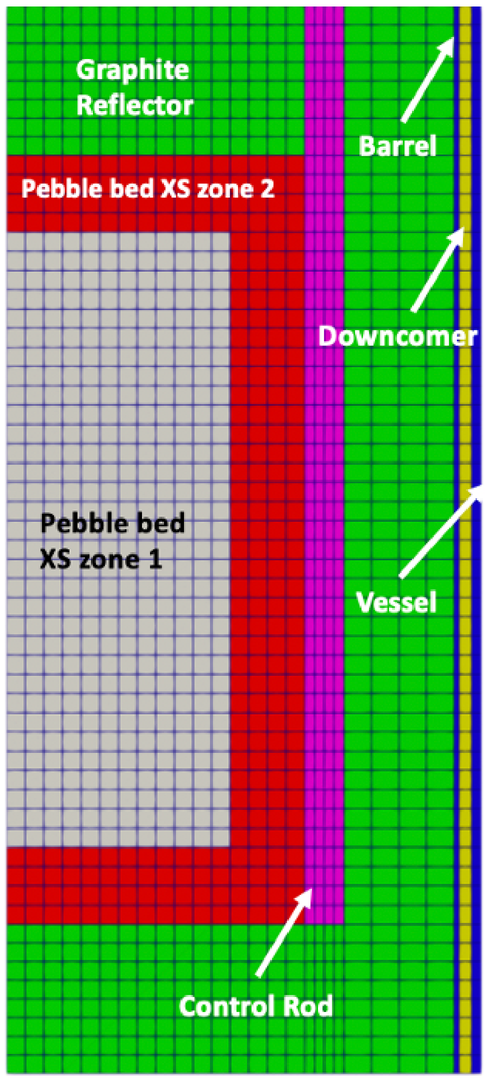

(a) Cross-section regions

Figure 4: gFHR Griffin equilibrium core mesh

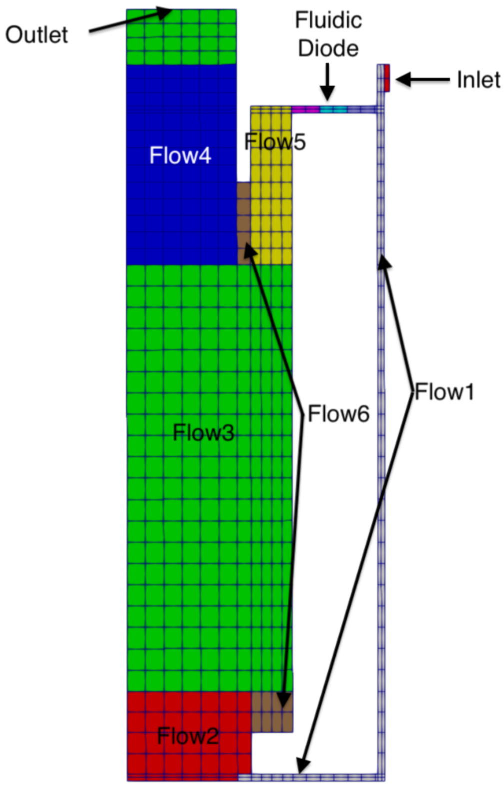

(a) Porous medium mesh

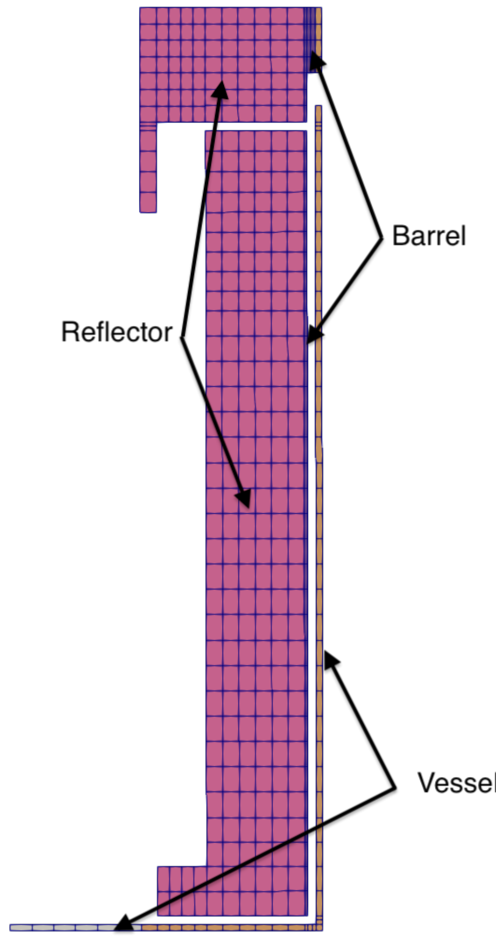

(b) Solid conduction mesh

Figure 5: gFHR Pronghorn thermal fluids mesh (figure courtesy of [14]).

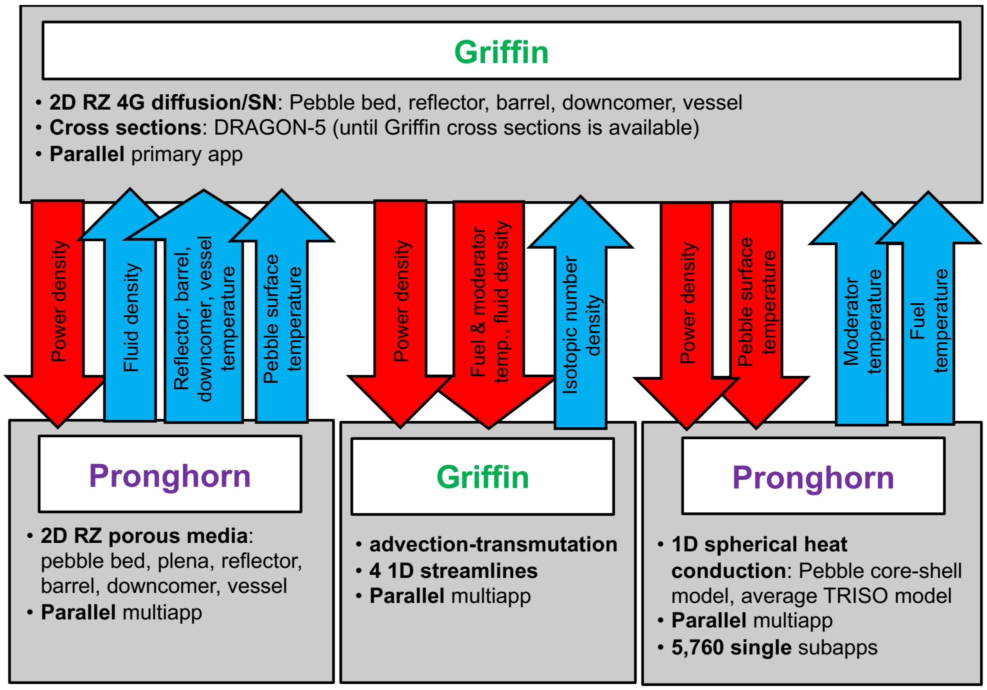

Figure 6: Multiphysics coupling for the gFHR equilibrium core calculation (figure courtesy of [14]).

2.2.2 Control Rod Worth

The CR worth of the Griffin model is given in Figure 7. Unlike with the gPBR-200, the cusping effects are not visible, mainly because the difference in cross-sections between boron carbide (B_4C) and FLiBe is less pronounced than that between B_4C and helium. The total rod worth, around 4,000 pcm, is also much smaller than in the gPBR-200 model.

2.3 Workflow

2.3.1 Hot Full-Power

This workflow (summarized in Figure 8) is very similar for both the gPBR-200 and gFHR when it comes to CRW and CRE simulations that start at nominal conditions. Specifically, it entails the following steps:

1. Cross-section generation: To perform a Griffin pebble depletion calculation, microscopic cross sections are needed. These are generated using DRAGON [2, 11] separately for the pebble and CR regions. The fuel cross-sections are tabulated based on burnup, fuel and

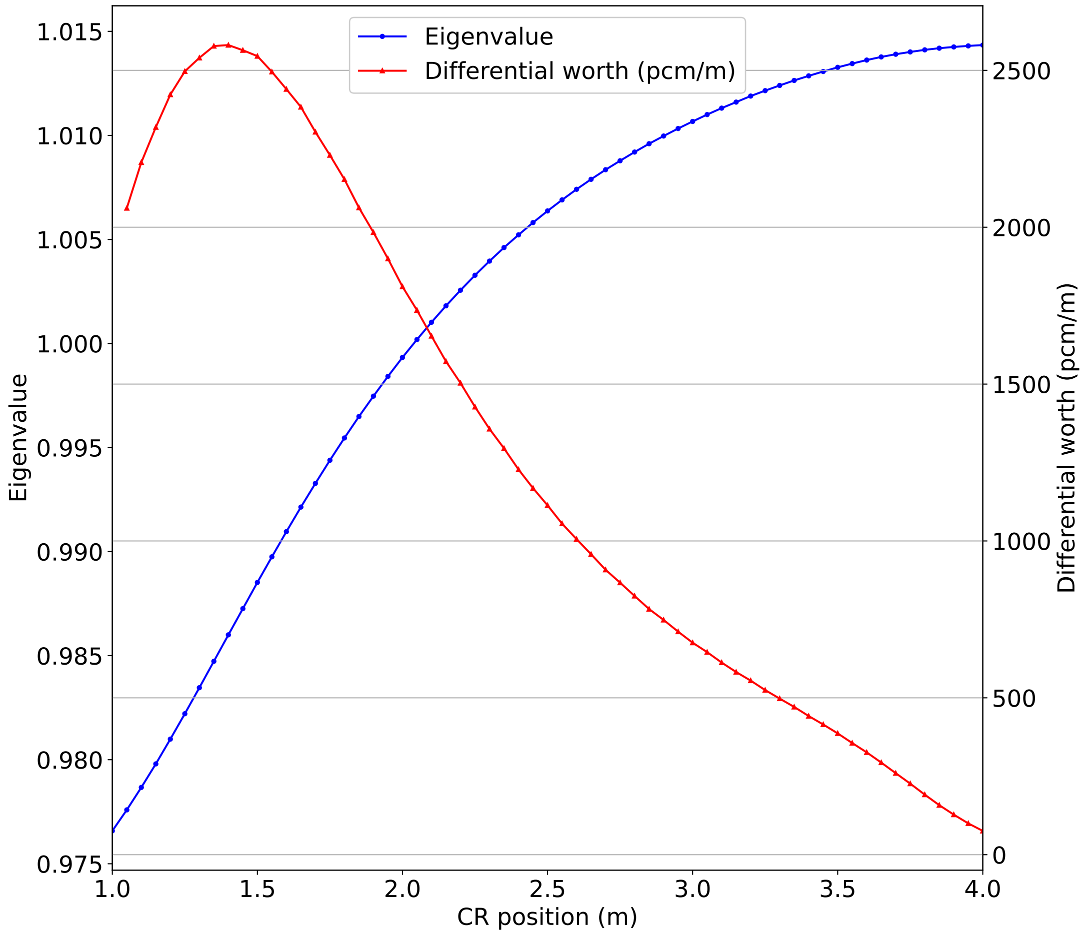

Figure 7: Reactivity curve of the gFHR model under hot full-power conditions.

moderator temperatures, and, for the gFHR model, coolant density. For the gPBR-200, directional diffusion coefficients are generated for the upper cavity using Serpent.

2. Griffin-Pronghorn equilibrium core calculation: The calculations described by Figures 2 and 6 are performed. Open convergence, the steady-state flux and temperature distributions, and pebble equilibrium isotopics corresponding to the hot full-power conditions are obtained via the equilibrium core depletion algorithm in Griffin [17].

3. Griffin adjoint calculation: Optionally, if the kinetics parameters (e.g., dynamic reactivity and reactor period) are desired during the transient, a standalone Griffin adjoint calculation

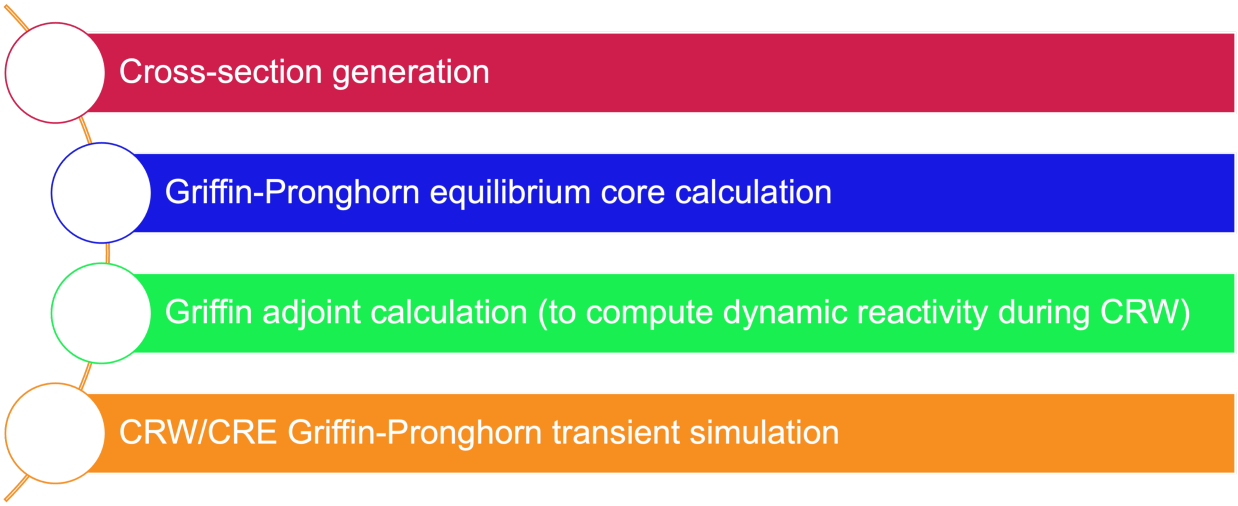

Figure 8: CRW/CRE workflow when starting from hot full-power conditions.

can be conducted based on the temperature field and isotopics obtained from the hot full-power steady-state solution.

4. CRW/CRE Griffin-Pronghorn transient simulation: Starting from the hot full-power steady-state solution, the CRs are moved per a prescribed delay and speed until they reach the final desired position.

2.3.2 Cold Zero-Power

This scenario only applies to the gPBR-200, as the gFHR model uses FLiBe, which should not be allowed to reach cold temperatures (e.g., below 750 K), as it could freeze. Because PBRs do not begin operation with fuel pebbles, there is very little (if any) excess reactivity the first time the reactor is started. The assumed sequence is thus that the core had been operating in equilibrium conditions, that it was shut down long enough for the poisons to saturate, and that the inadvertent CR motion occurred right before the reactor was restarted. During this time, the shutdown rods are not inserted into the core and the mechanism to insert them fails. While concurrent failure of the shutdown rod mechanism and inadvertent CR motion is highly improbable, the combination of these two events provides a bounding case, with maximum reactivity insertion.

The workflow, summarized in Figure 9, is similar to that for the hot full-power case, but with a few additional steps:

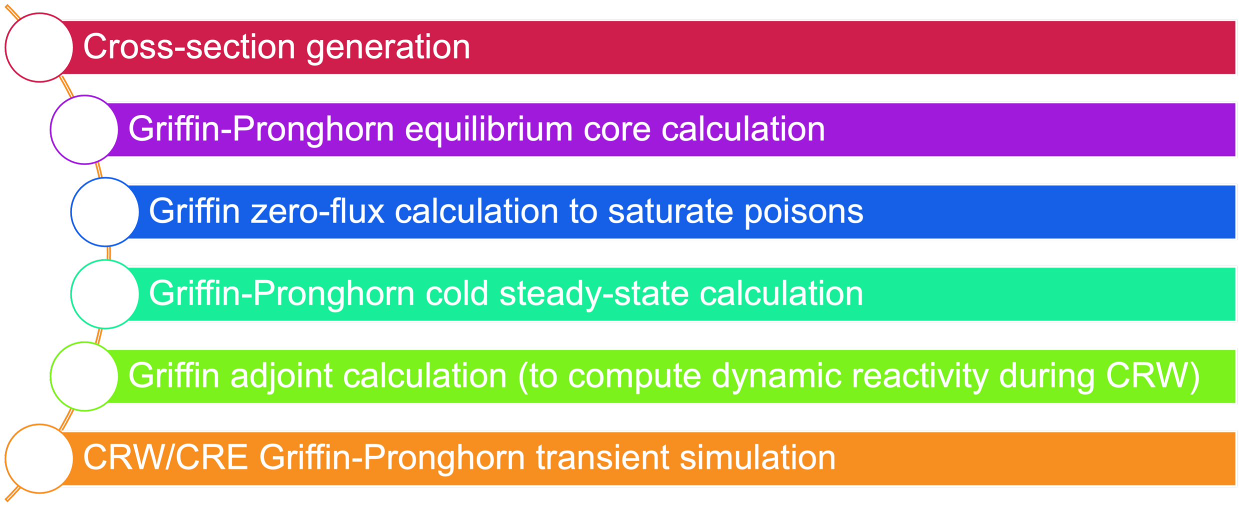

Figure 9: CRW/CRE workflow when starting from cold zero-power conditions.

1. Cross-section generation: Same as for the hot full-power case.

2. Griffin-Pronghorn equilibrium core calculation: Same as for the hot full-power case.

3. Griffin zero-flux calculation: The pebble isotopics are restarted from the hot full-power steady-state solution and then depleted for 7 days to saturate (long enough to saturate xenon and samarium) at near-zero power.

4. Griffin-Pronghorn cold steady-state calculation: The power is maintained at a very low value, and the cold steady-state fluxes and temperature are obtained.

5. Griffin adjoint calculation: Optionally, a standalone Griffin adjoint calculation is conducted based on the temperature field and isotopics that correspond to the cold zero-power steady-state solution.

6. CRW/CRE Griffin-Pronghorn transient simulation: Starting from the cold zero-power steady-state solution, the CRs are moved per a prescribed delay and speed until they reach the final desired position.

2.4 Transient Specifications

The transient specifications for the various scenarios considered in this work are summarized in Table 1. Four cases are considered: CRW and CRE events starting from cold and hot conditions.

The CR speeds for the CRW and CRE events were chosen so as to be consistent with the PBMR-400 benchmark [13]. The reactivity insertions were approximately (but conservatively) determined using a gPBR-200 equilibrium core 3-D Serpent model. In making comparisons between gas- and fluoride-cooled PBRs, the same reactivity insertions were also used for the gFHR model. To model the smaller reactivity insertions for the CRE events, the same initial rod position was assumed, but the CRs were stopped once the desired reactivity was inserted.

Table 1: Transient specifications for the CRW and CRE events considered in this work.

Event	Number of CRs	Initial State	CR Speed	Approximate Reactivity Insertion
CRW	All	Hot full-power	1 cm/s	500 pcm
CRW	All	Cold zero-power*	1 cm/s	9,000 pcm
CRE	1	Hot full-power	Ejection in 0.1 s	100 pcm
CRE	1	Cold zero-power*	Ejection in 0.1 s	500 pcm

*: gPBR-200 only

3. NUMERICAL RESULTS

The transient results for the gPBR-200 and gFHR models are presented in Sections 3.1 and 3.2, respectively.

3.1 Gas-cooled Pebble-Bed Reactor

3.1.1 Hot Full-Power Control Rod Withdrawal

For this transient, the core is assumed to have been operating at full power and to be in equilibrium. After 1 second (to test whether the initial condition is indeed in equilibrium), all the rods are removed at a speed of 1 cm/s. Figure 10 summarizes the evolution of the power and temperature for the first several minutes. Although the CRs are slowly removed, most of the reactivity insertion occurs within the first minute, due to the rods being only shallowly inserted. The power rapidly increases from 200 MW to almost 290 MW after 20 seconds, at which point the strong temperature feedback starts bringing the power back down. Eventually, the power and the core temperature stabilize to values exceeding their initial values in order to compensate for the positive reactivity added by the CR removal. The maximum fuel temperature is increased by more than 50 K but remains under 1200 K (i.e., far below any temperature limit [on the order of 2100 K for TRISO fuel]).

3.1.2 Hot Full-Power Control Rod Ejection

This transient is similar to the previous one; however, the CRs do not insert as much reactivity but are instead removed almost instantaneously. The CR motion is initiated after 0.1 seconds (to test whether the initial condition is indeed in equilibrium) and is completed after 0.2 seconds. As shown in Figure 11, the power increases much faster, peaking at around 248 MW within 4 seconds of the CRE event. The power then starts decreasing, and it stabilizes at around 205 MW (i.e., at a lower level than for the CRW event, since the amount of reactivity needing to be compensated for is smaller). Likewise, the rise in the fuel and graphite temperatures is more limited and thus does not threaten the integrity of the TRISO fuel.

3.1.3 Cold Zero-Power Control Rod Withdrawal

For this transient, the core is assumed to be critical at near-zero power, and in thermal equilibrium. After 1 second, all the rods are removed at a speed of 1 cm/s. The difference with Section 3.1.1 is that the core components are much colder (around 533 K) (i.e., much further from any temperature limit), but the total reactivity to be inserted is much larger (around 15 $). The initial power is assumed to be 1 W, thereby neglecting any decay heat. Because of the slow CR motion, this reactivity is inserted over the course of almost 14 minutes. As shown in Figure 12, the power increases extremely fast in the first 20 seconds, as the power is still too low for any temperature feedback to be perceptible. The power then peaks at around 240 MW before being brought back down by the reactivity feedback driven by the rapid temperature increase. However, it does not stabilize to a lower power, as the CRs are still being removed. As a result, the power and temperature continue to rise until the CRs are mostly removed from the core. At that point, the power stabilizesat around 465 MW—more than double the nominal power value. However, after the transient has lasted for more than 10 minutes, the fuel temperature reaches values barely below 1,900 K—which is only a few hundred degrees from the fuel temperature limit—before stabilizing around 1850 K.

The oscillations in the power curve stem from the cusping effect seen in Figure 3. This effect

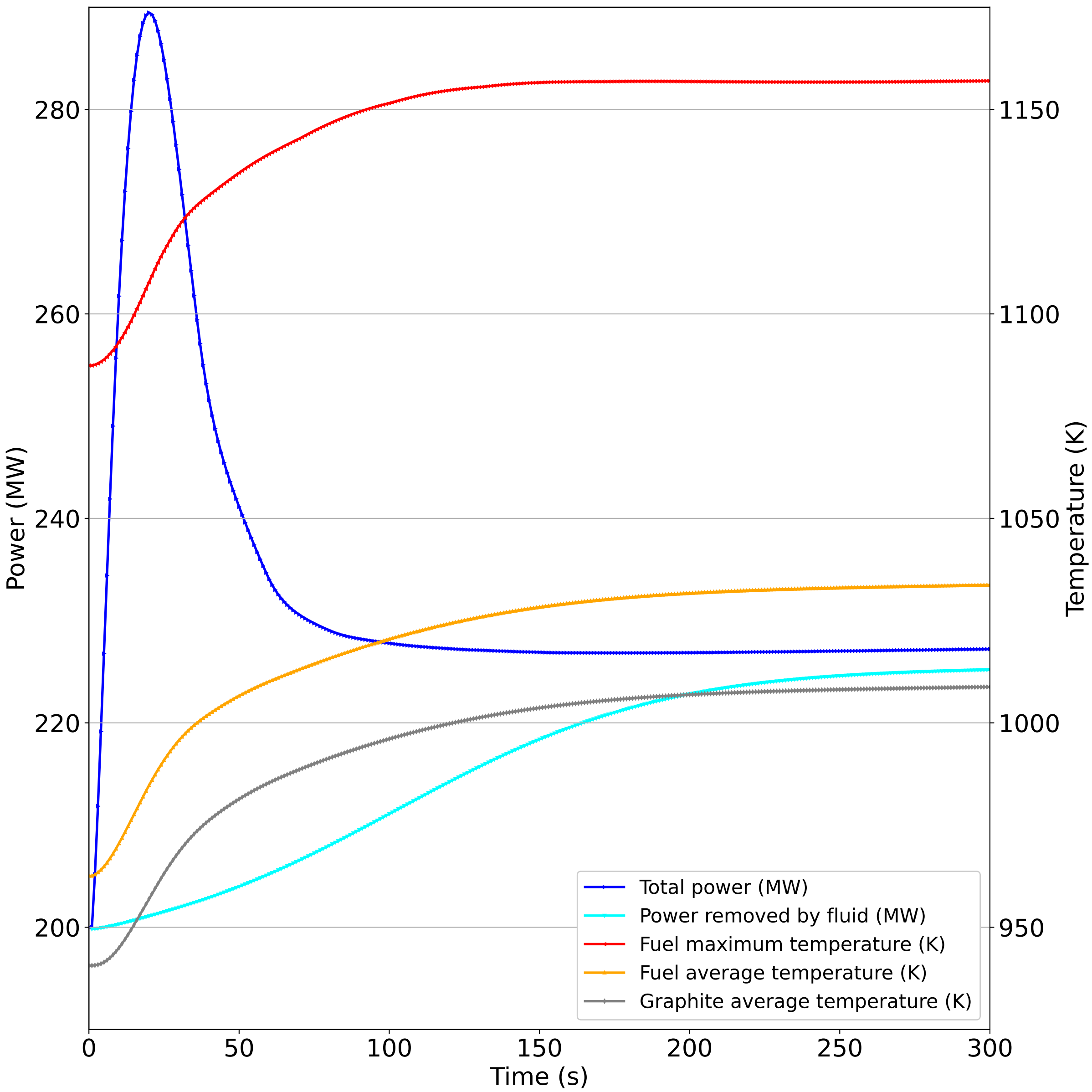

Figure 10: CRW simulation for the gPBR-200 model starting from hot full-power conditions.

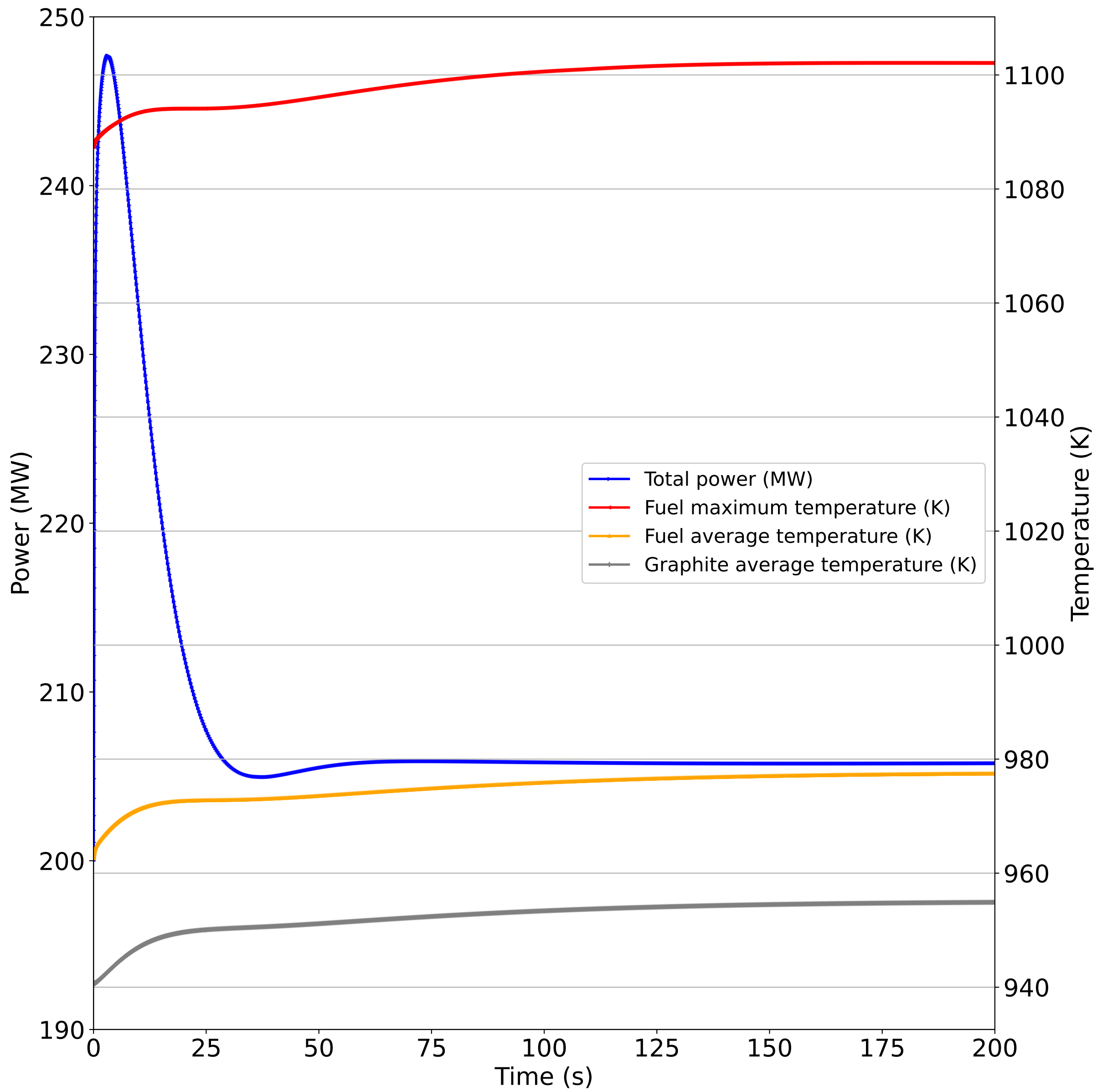

Figure 11: CRE simulation for the gPBR-200 model when starting from hot full-power conditions.

manifests itself as non-smoothness in the reactivity curve, as the tip of the CR does not align with the mesh. This becomes especially visible when the CRs are being moved slowly, such as during CRW events.

3.1.4 Cold Zero-Power Control Rod Ejection

This transient is similar to the previous one, except that the CRs do not insert as much reactivity but are instead removed almost instantaneously. The CR ejection is performed in 0.1 seconds, following a 1-second delay to test whether the initial condition is indeed in equilibrium. The large amount of reactivity insertion multiplies the power by almost eight orders of magnitude over the first 20 seconds, reaching almost 92 MW. The rapid rise in core component temperatures prevents the power from exceeding that, and quickly drops it back to below 20 MW. During the whole simulation, the maximum fuel temperature remains below 630 K—a temperature easily withstood by the TRISO fuel.

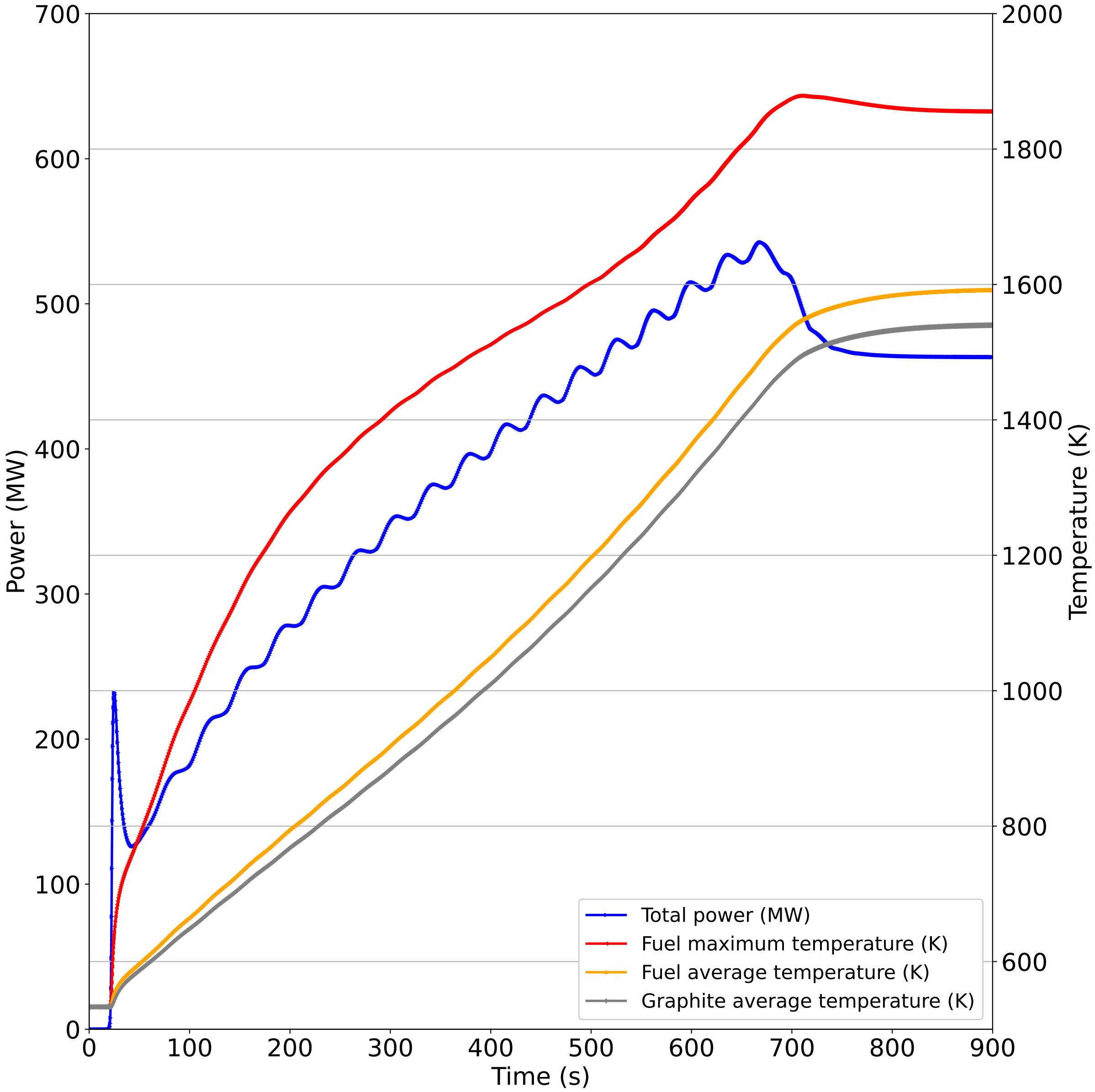

Figure 12: CRW simulation for the gPBR-200 model when starting from cold zero-power conditions.

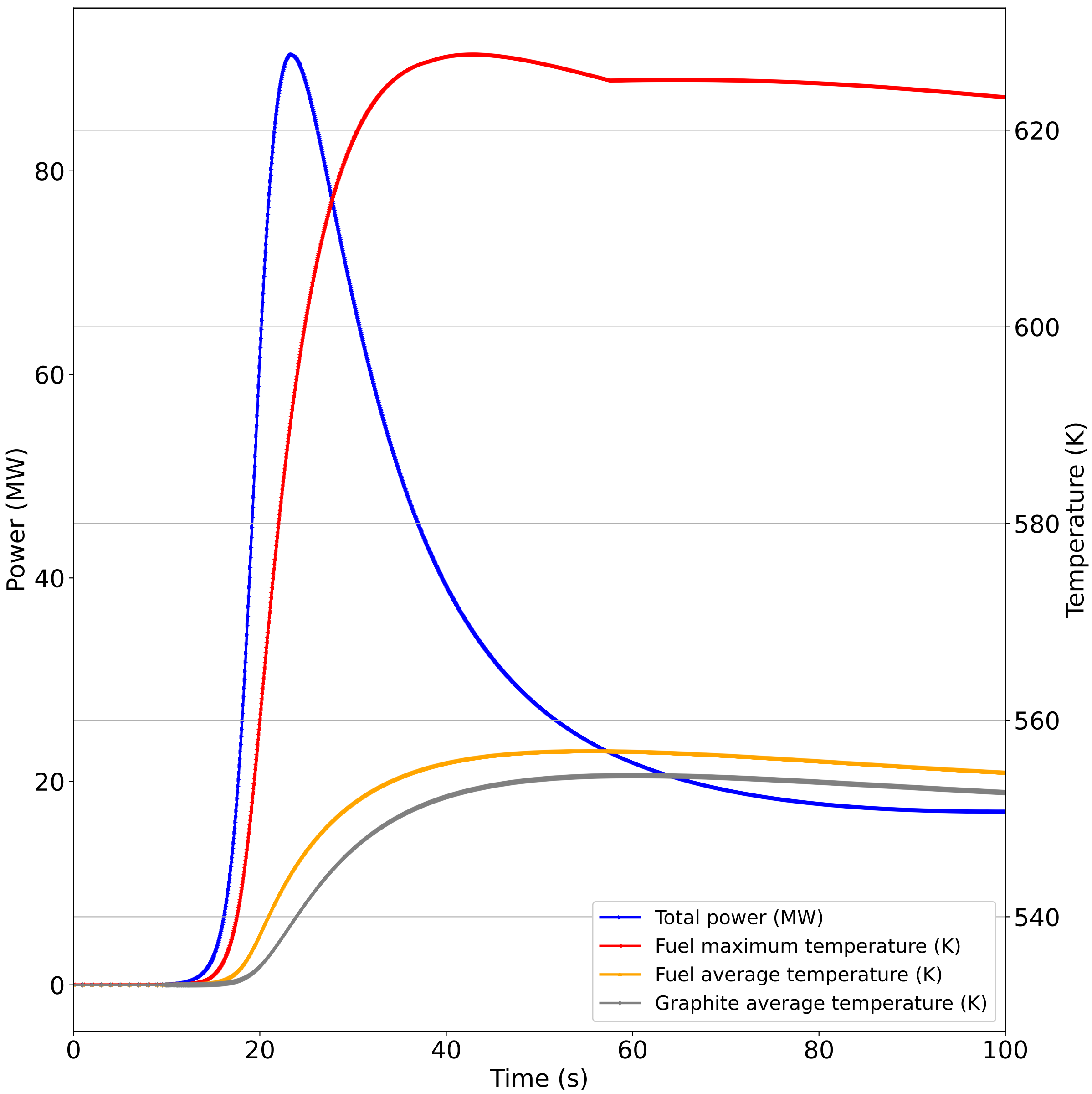

Figure 13: CRE simulation for the gPBR-200 model when starting from cold zero-power conditions.

3.2 Fluoride-cooled Pebble-Bed Reactor

This section presents numerical results for the gFHR model described in Section 2.2. The cold zero-power transients are not considered, given that the coolant would freeze in cold conditions. To compare the behavior with the gPBR-200 model, the same reactivity insertion shown in Table 1 is added (i.e., around 100 and 500 pcm for the CRW and CRE events, respectively). Future work will include adding the CRs to the gFHR Serpent model in order to evaluate whether these insertions are representative of a PB-FHR.

3.2.1 Hot Full-Power Control Rod Withdrawal

For this simulation, the core is assumed to have been operating at full power and to be in equilibrium. After 1 second (to test whether the initial condition is indeed in equilibrium), all the rods are removed at a speed of 1 cm/s. Given the initial position of the CRs, it takes about 100 seconds for them to be fully withdrawn. Figure 14 summarizes the core's response to this CRW event: the power increases significantly from 280 to almost 500 MW in a few minutes, but unlike in the gPBR case, no overshoot—characterized as a temporary spike before stabilizing to a lower value—in power is observed. This is mainly thanks to the larger power density of the core, implying that, for a given nominal power, the thermal capacitance of the reactor is lower. Therefore, the core heats up faster and the temperature feedback occurs before the power has time to increase significantly. By the end of the simulation, the fuel maximum temperature is below 1150 K, which is—once again—not a concern given the typical temperature limit for TRISO fuel.

3.2.2 Hot Full-Power Control Rod Ejection

This transient is similar to the previous one, except that only one-fifth of the reactivity is inserted. However, this insertion is performed almost instantaneously. The results, summarized in Figure 15, exhibit a small power overshoot within the first few seconds, with the power reaching almost 324 MW before dropping back down and then stabilizing at around 320 MW. This overshoot occurs for this CRE event because of the rapidity of the reactivity insertion, but remains fairly limited (compared to, for instance, the gPBR-200 CRE event shown in Figure 11). The increase in fuel and graphite temperatures is also limited (less than 50 K over the entire

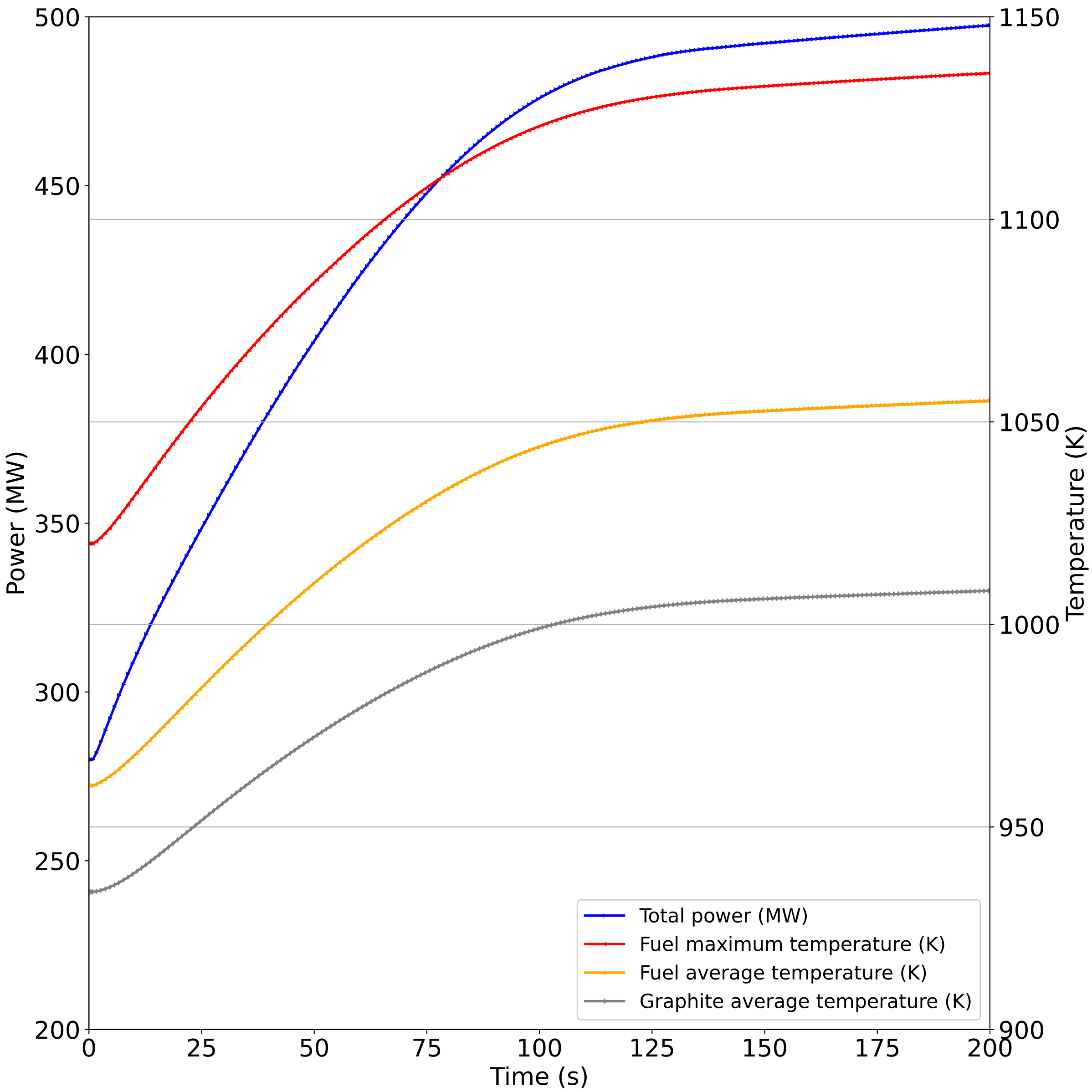

Figure 14: CRW simulation for the gFHR model when starting from hot full-power conditions.

transient).

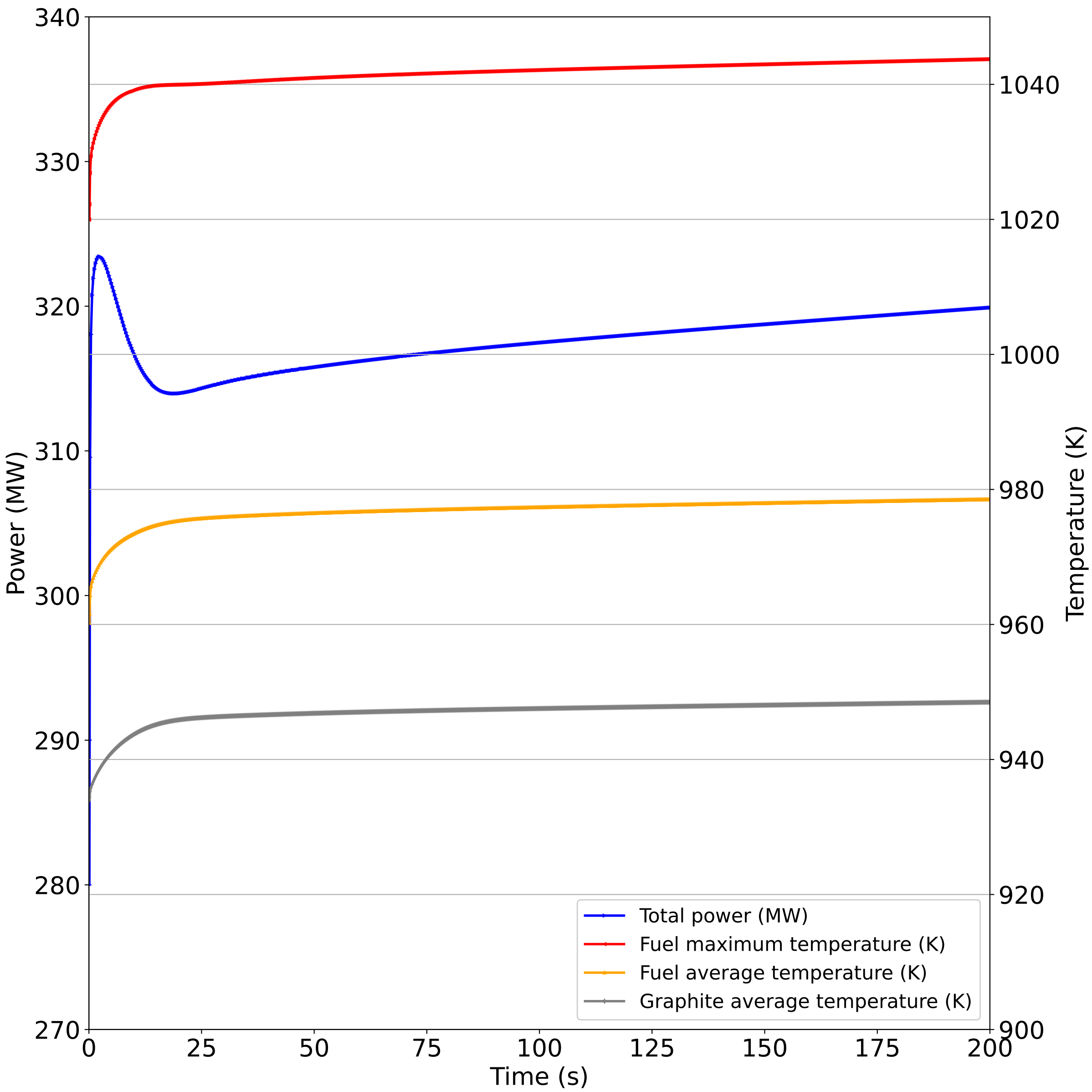

Figure 15: CRE simulation for the gFHR model when starting from hot full-power conditions.

4. CONCLUSIONS AND RECOMMENDATIONS

4.1 Conclusions

In summary, the responses of a generic gas- and a fluoride-cooled PBR concept—the gPBR-200 and gFHR, respectively—during reactivity insertion accidents were studied. Both models rely on 2-D axisymmetric simulations to solve the neutron flux distribution, isotopics, and temperature across the core—in addition to numerous representative pebble and TRISO simulations to determine fuel and moderator temperatures. This not only allows for computing maximum temperatures in the core—thereby estimating how near to operational/safety limits the fuel might get—but also predicting how much of the core exceeds a given temperature limit, as well as local energy deposition rate.

These models considered both CRW and CRE events. The former introduces a great deal more reactivity, as all the CRs are withdrawn (as opposed to only a single one being withdrawn for the CRE), though at a much slower pace. In addition, for the gPBR-200, two limiting cases were considered, with the core starting under both hot full-power conditions and cold zero-power conditions. While the amount of reactivity added in the latter case was much higher (due to the much lower temperatures and the lack of neutron poisons such as Xe-135), the margin to temperature limits was also far more significant.

Overall, for the design considered, none of the accidents resulted in the maximum fuel temperature reaching values close to the TRISO limit. However, the methodology presented herein could be very relevant if some designs consider reduced conservatisms (e.g., higher temperatures) to achieve enhanced economics.

4.2 Future Work

The following is a non-exhaustive list of the tasks planned to be performed to improve the models:

- Improve the CR model by reducing the cusping effects (for the gPBR-200 model) and enhancing the CR differential worth, especially as the tip of the CR nears the upper cavity. Potential paths forward include using a transport solver (to afford better behavior inside the void region) and increasing the amount of axial elements used in the CR region (to reduce cusping). A 3-D model would also enable capturing the azimuthal dependency of the neutron flux, introduced by the positions of the CRs.

- Incorporate a fuel performance model to estimate TRISO failure probabilities. While initial models would likely be limited to considering pressure vessel failure—which would largely be determined by the maximum temperature over the course of the transient—more elaborate models could be pursued as well [3], e.g., to account for fluence, burnup and manufacturing uncertainties.

- A study similar to that done in [7] could be performed on this model in order to evaluate the impact of various parameters on TRISO failure probabilities.

5. Acknowledgments

This manuscript was authored by Battelle Energy Alliance, LLC under contract no. DE-AC07-05ID14517 with the U.S. Department of Energy. The U.S. Government retains and the publisher, by accepting the article for publication, acknowledges that the U.S. Government retains a nonexclusive, paid-up, irrevocable, worldwide license to publish or reproduce the published form of this manuscript, or allow others to do so, for U.S. Government purposes.

This research was funded by the U.S. Department of Energy Advanced Reactor Technologies Program for Gas Cooled Reactors (ART-GCR). It made use of the resources of the High Performance Computing Center at Idaho National Laboratory, which is supported by the Office of Nuclear Energy of the U.S. Department of Energy and the Nuclear Science User Facilities under contract no. DE-AC07-05ID14517.

The authors would like to recognize John Shaver for his excellent and prompt technical review of this manuscript.

REFERENCES

[1] Balestra, Paolo, Schunert, Sebastian, Carlsen, Robert W, Novak, April J, DeHart, Mark D, and Martineau, Richard C, Pbmr-400 benchmark solution of exercise 1 and 2 using the moose

based applications: Mammoth, pronghorn, *EPJ Web Conf.*, *247*, 06,020, doi:10.1051/epjconf/202124706020, 2021.

[2] Chambon, R., HTR10 Modeling with DRAGON & DONJON, *Tech. rep.*, Ecole Polytechnique of Montreal, 2019.

[3] Dhulipala, S. L., et al., Accelerated statistical failure analysis of multifidelity triso fuel models, *Journal of Nuclear Materials*, *563*, 153,604, doi:https://doi.org/10.1016/j.jnucmat.2022.153604, 2022.

[4] Ghezzi, C. G., and N. R. Brown, Triso burnup-dependent failure analysis in fhrs using bison, *Journal of Nuclear Materials*, *586*, 154,651, doi:https://doi.org/10.1016/j.jnucmat.2023.154651, 2023.

[5] Giudicelli, G., A. Lindsay, P. Balestra, R. Carlsen, J. Ortensi, D. Gaston, M. DeHart, A. Abou-Jaoude, and A. J. Novak, Coupled multiphysics transient simulations of the mk1-fhr reactor using the finite volume capabilities of the moose framework, in *Mathematics and Computation for Nuclear Science and Engineering*, American Nuclear Society, 2021.

[6] Giudicelli, G. L., A. D. Lindsay, R. Freile, and J. Lee, NEAMS-TH-CRAB, *Tech. Rep. INL/EXT-21-62895*, Idaho National Laboratory, 2021.

[7] Gorton, J. P., and N. R. Brown, Defining the performance envelope of reactivity-initiated accidents in a high-temperature gas-cooled reactor, *Nuclear Engineering and Design*, *370*, 110,865, doi:https://doi.org/10.1016/j.nucengdes.2020.110865, 2020.

[8] Jung, Y., and C. Lee, PROTEUS-MOC user manual, *Tech. Rep. ANL/NE-18/10*, Argonne National Laboratory, 2018.

[9] Leppänen, J., Serpent– a continuous-energy Monte Carlo reactor physics burnup calculation code., *Tech. rep.*, VTT Technical Research Centre of Finland, 2015.

[10] Liu, Z., K. Smith, B. Forget, and J. Ortensi, Cumulative migration method for computing rigorous diffusion coefficients and transport cross sections from monte carlo, *Annals of Nuclear Energy*, *112*, 507–516, doi:https://doi.org/10.1016/j.anucene.2017.10.039, 2018.

[11] Marleau, G., A. Hebert, and R. Roy, A user guide for dragon version5, *Tech. Rep. IGE–335*, Ecole Polytechnique de Montreal, 2020.

[12] Mulder, E. J., and W. A. Boyes, Neutronics characteristics of a 165 MWth Xe-100 reactor, *Nuclear Engineering and Design*, *357*, 110,415, doi:https://doi.org/10.1016/j.nucengdes.2019.110415, 2020.

[13] NEA, PBMR Coupled Neutronics/Thermal-Hydraulics Transient Benchmark: The PBMR-400 Core Design - Volume 1: The Benchmark Definition,, *Tech. rep.*, OECD Publishing, Paris, 2013.

[14] Ortensi, J., C. Mueller, S. Terlizzi, G. L. Giudicelli, and S. Schunert, Fluoride-cooled high-temperature pebble-bed reactor reference plant model, doi:10.2172/1983953, 2023.

[15] Pope, M. A., Transmutation analysis of enriched uranium and deep burn high temperature reactors, *Tech. Rep. INL/EXT-12-26423*, Idaho National Laboratory, 2012.

[16] Schunert, S., Y. Wang, J. Ortensi, V. M. Labouré, F. N. Gleicher, M. D. DeHart, and R. C. Martineau, Control rod treatment for fem based radiation transport methods, *Annals of Nuclear Energy*, *127*, 293–302, doi:10.1016/j.anucene.2018.11.054, 2019.

[17] Schunert, S., J. Ortensi, Y. Wang, P. Balestra, M. Jaradat, O. Calvin, J. Hanophy, and L. Harbour, An equilibrium core depletion algorithm for pebble-bed reactors in the griffin code, *Annals of Nuclear Energy*, *192*, 109,980, doi:https://doi.org/10.1016/j.anucene.2023.109980, 2023.

[18] Stewart, R., P. Balestra, D. Reger, and E. Merzari, Generation of localized reactor point kinetics parameters using coupled neutronic and thermal fluid models for pebble-bed reactor transient analysis, *Annals of Nuclear Energy*, *174*, 109,143, doi:https://doi.org/10.1016/j.anucene.2022.109143, 2022.

[19] Stewart, R., P. Balestra, D. Reger, and G. Strydom, Novel pebble shuffling capabilities to generate reduced order models training databases, *Tech. Rep. INL/RPT-22-68918*, Idaho National Laboratory, 2022.

[20] Wang, Y., et al., Rattlesnake: A MOOSE-based multiphysics multischeme radiation transport application, *Nuclear Technology*, *207*(7), 1047–1072, doi:10.1080/00295450.2020.1843348, 2021.